Experimental Study of Cavitation in Laminar Flow

[1]Kilian Croci *; [1]Florent Ravelet; [1]Jean-Christophe Robinet; [2]Amélie Danlos

[1]*DynFluid Laboratory, Arts et Métiers PariTech, Paris, FRANCE; [2] DynFluid Laboratory, Conservatoire National des Arts et Métiers, Paris, FRANCE*

Abstract

An experimental set-up has been especially developed in order to observe cavitation in laminar flows. Experiments have been carried out with a silicon oil of viscosity $\upsilon = 100\ cSt$ passing through a Venturi-type geometry with 18°/8° convergent/divergent angles respectively. The range of Reynolds numbers at the inlet section is between 350 and 1000. For these flow conditions, the Venturi only experiences air releasing gaseous cavitation for which two dynamic regimes are identified. They are characterized by two critical Reynolds numbers, induced by major hydrodynamic changes in the flow, in addition to a hysteresis effect between the inception and the disappearance of cavitation.

Keywords: laminar flows; gaseous cavitation regimes; cavitation inception; bubbles; hysteresis

1. Introduction

Several regimes can occur in turbulent cavitating flows. In studies about water flows coming across obstacles, and in particular with Venturi geometries, four main cavitation regimes can be identified:

- An **intermittent regime** which corresponds to the cavitation inception. This regime occurs for relatively high pressures and is characterized by the intermittent inception and the implosion [1] of small vapor bubbles at the Venturi throat.
- For lower pressure conditions a **"closed cavity" regime**, presenting relatively stable vapor/liquid mixture cavities, is observed. Re-entrant jets, induced by a recirculation flow, occur at the cavity rear inducing the mixing of liquid and vapor without cloud shedding.
- A **transient regime** of **partial cavitation** [2] is obtained decreasing the pressure in the test section. This highly unsteady regime is characterized by several cloud cavitation shedding dynamics induced respectively by: the re-entrant jet and by the periodical condensations and implosions of coherent cloud cavitation structures named condensation shock wave [3].
- For really low pressure conditions, cavities can reach important sizes and a **periodic regime** (also called **supercavitation**) can be established [4]. In this particular regime the condensation shock wave, which occurs periodically, is the dominant shedding dynamic in the flow.

These regimes and shedding mechanisms still remain of principal interest both experimentally and numerically. However cavitation flows have, to the authors' knowledge, been very little investigated using fluids with high-viscosity [5]. The present study focuses on the different cavitation regimes observed in laminar flows. Two gaseous cavitation regimes are highlighted and a comparison is made with the turbulent regimes previously presented. The paper is organized as follow: first the experimental set-up is described in §2. The cavitation regimes are then highlighted (§3) and finally conclusions and perspectives are proposed in §4 and §5.

2. Experimental Set-up

The experiments are conducted in a closed test loop where a pump impels a silicone oil flow with a flow rate from 21 to 60 $L.min^{-1}$. The Bluesil FLD 47 V100® silicone oil main characteristics are given in Table 1.

Viscosity υ $(m^2.s^{-1})$	10^{-4}
Volumic Mass ρ $(kg.m^{-3})$	965
Vapor Pressure P_v (Pa)	1.33
Surface Tension S $(N.m^{-1})$	20.9×10^{-3}

Table 1 - Characteristics of Bluesil FLD 47 V100® silicone oil at $25°C$ given by the constructor.
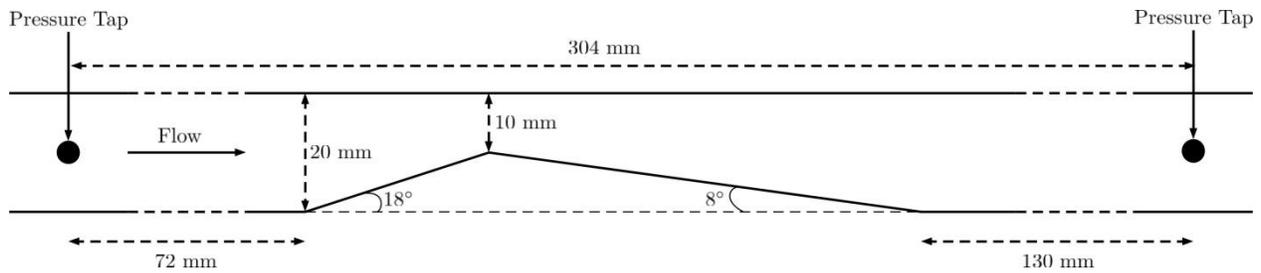
*Corresponding Author, Kilian Croci: kilian.croci@ensam.eu

Figure 1 – Venturi geometry sketch. The width of the test section is $10\ mm$ and the height at the inlet section $h_{in} = 20\ mm$.

The test section is represented in figure 1. It consists of a rectangular inlet section of width $10\ mm$ and height $20\ mm$ and a $10 \times 10\ mm^2$ square section at the throat. The Venturi-type geometry presents $18°/8°$ convergent/divergent angles respectively. The velocity is measured with an ultrasonic flow-meter and studied for $1.75 < U_{in} < 5.00\ m.s^{-1}$ at the inlet test section corresponding to Reynolds numbers ($Re = \frac{U_{in} \times h_{in}}{v}$) taken from 350 to 1000. In the meantime the pressure is measured in the test section upstream (P_{in}) and downstream (P_{out}) of the throat. The cavitation number, such as the Reynolds number, is defined at the beginning of the test section as follow: $\sigma = \frac{P_{in} - P_v}{1/2 \rho U_{in}^2}$. Finally, the temperature is measured with a PT100 sensor and the kinematic viscosity v is reevaluated accordingly based on our own calibration. In the following parts of the study a laminar flow description is introduced (figure 2) and the inception, in addition to the different cavitation regimes, will be presented and characterized as a function of the cavitation and the Reynolds numbers in the figure 3.

3. Cavitation Inception

The inception of cavitation, widely studied into water, is an intricate phenomenon which depends on several parameters. As explained in the works of Brennen [4], it might depend on the water quality regarding on the dissolved and the free gas content. For a saturated liquid experiencing a low pressure region, important outgassing and vaporization may occur in the flow generating the intermittent regime described in §1. Moreover when a nucleus goes through a region with a critical pressure drop in the surrounding liquid, its radius would be able to grow unboundedly.
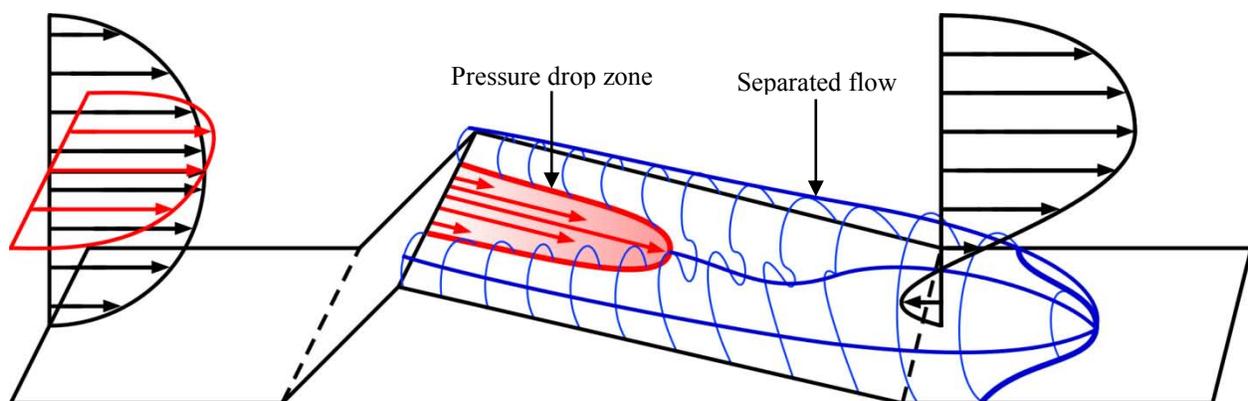

Figure 2 – Sketch of the flow at the inception. The flow separation occurs at relatively low Reynolds numbers in non-cavitating flows but when an adverse pressure gradient is generated near this region, the growth and capture of air bubbles become possible leading to attached air cavities and recirculating bubbles.

Such as in a turbulent water-flow a low pressure region can be generated in a laminar flow, inducing outgassing and nuclei explosive growths. In a Venturi geometry the velocity, as well as the pressure drop, is maximum at the center of the throat. Consequently a large air bubble might be generated in this central region which is illustrated in figure 2. After this inception, the bubble is carried away by the stream and, contrary to the water-flows, does not implode because of the high viscosity of the oil. A part of the air bubble can then be captured by the separated zone

downstream of the Venturi throat which is already present in the non-cavitating flow at low Reynolds number. In summary for a critical Reynolds number Re_c^i, an adverse pressure gradient can be generated leading to an explosive bubble growth near the separated region. The recirculation region can then captures a part of the expanded bubble and make it reach back to the Venturi throat on one wall-side. After a few repetitions of this cycle, two elongated "tadpole shape" bubbles settle on both side-wall at the Venturi throat.

As a result the cavitation inception, previously defined, occurs above a critical inlet Reynolds number $Re_c^i \approx 650$ and depends on the cavitation number. The inception conditions ($Re = f(\sigma)$) are exposed in figure 3 with the blue curve. Under this curve, a dynamic regime can be defined: the **bubbly recirculation regime**, characterized by bubbles' inception and recirculation to the wall-sides of the Venturi throat. For lower Reynolds numbers and higher cavitation numbers, the recirculation regime disappears but not the two tadpole bubbles at the throat which oscillate with micro-bubble sheddings until a critical desinent Reynolds number $Re_c^d \approx 350$. It defines a second regime called the **tadpole regime**.
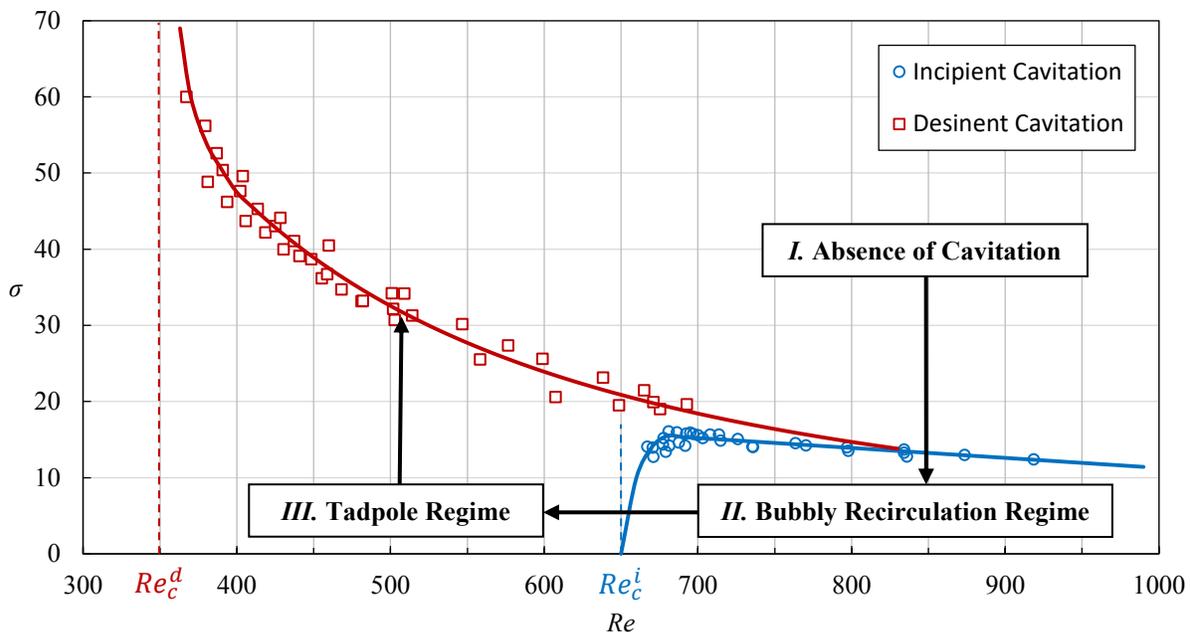
4. Cavitation Regimes

Figure 3 – Map of the dynamic regimes as a function of Reynolds and cavitation numbers. The blue and the red curves correspond repectively to the inception and to the desinence of cavitation. The blue dotted line denotes the inception critical Reynolds number Re_c^i whereas the red dotted line represents the desinent critical Reynolds number Re_c^d. The cycle of cavitation hysteresis is defined as follow. *I* : Absence of cavitation; (decreasing the cavitation number) *II* : Inception of cavitation and bubbly recirculation regime; (decreasing the Reynolds number) *III* : Subcritical tadpole regime and disappearance of cavitation when the cavitation number is enough increased. The uncertainties are estimated to 4 % for the Reynolds numbers and to 2% for the cavitation numbers.

The figure 3 shows the hysteresis between the inception and disappearance of cavitation with the two different cavitation regimes previously introduced. The two asymptotes, corresponding to the two critical Reynolds numbers characterized earlier, might be due to the recirculation flow characteristics. For Reynolds numbers higher than 650, the oil flow might be fast enough to generate a pressure drop zone at the throat and, in the meantime, the shear stress might be enough developed in order that a bubble generated at the throat get captured by a thick recirculation zone and go back to the Venturi throat. The desinent critical Reynolds number Re_c^d, which is around 350, might correspond to the disappearance of the recirculation zone. Near this condition, the two bubbles become less and less stable and symmetry breaks can often be observed.

Regarding to the figure 3, the two different regimes can be defined depending on the flow conditions. The **bubbly recirculation regime** is defined by the inception curve (occurring for $Re > Re_c^i$) for which the cavitation number slowly decreases with the Reynolds number. Under this curve, bubbles are generated at the throat, are carried away by the flow, get captured by the recirculation zone and its negative velocities and, finally, they reach the Venturi slope to the throat where they settle to one or the other wall-side. It results in the presence of two attached bubbles at both wall-side of the Venturi throat in addition to recirculating bubbles as illustrated in figure 4.
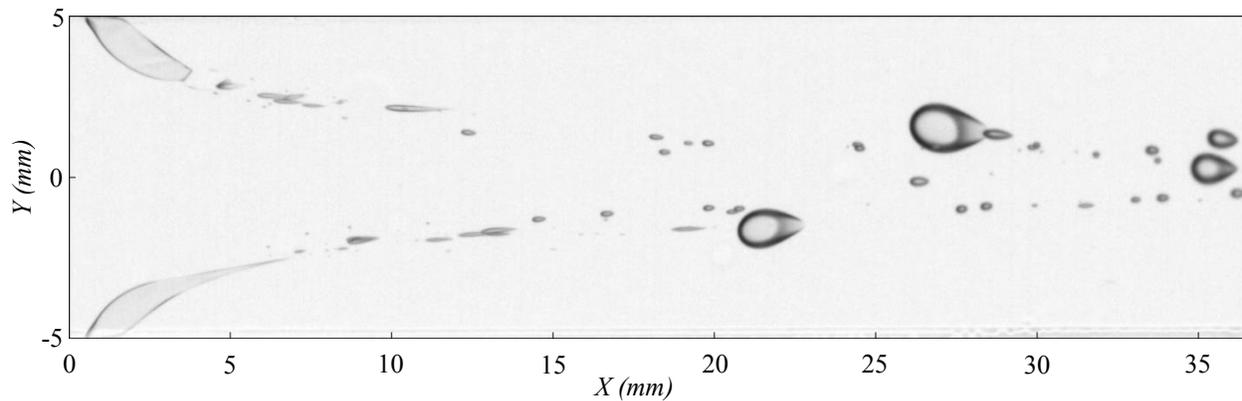

Figure 4 – Top view of the bubbly recirculation regime captured at $Re = 946$ and $\sigma = 8$. The oil stream is coming from the left to the right. The Venturi throat is positioned at $X = 0\ mm$. Dark regions are indicative for the contours of the bubbles. The two tadpole bubbles (left) are attached near the throat with micro-bubble shedding whereas recirculating bubbles (right) reach back the Venturi slope to the throat.

On the other hand the **tadpole regime** (figure 5) is the result of a hysteresis between inception and the disappearance of these two bubbles. Indeed after the settlement of the bubbles at the throat, they do not disappear immediately when the Reynolds number is decreased and the cavitation number is increased. However in these conditions the bubbly recirculation regime is stopped and only the two oscillating bubbles persist. The tadpole regime occurs for flow conditions which are below the desinent curve (red dots in figure 2) and is limited by the critical desinent Reynolds number Re_c^d. For Reynolds numbers $Re > Re_c^i$, the desinent curve seems to rejoin the inception curve meaning that in high velocity conditions the hysteresis disappears.
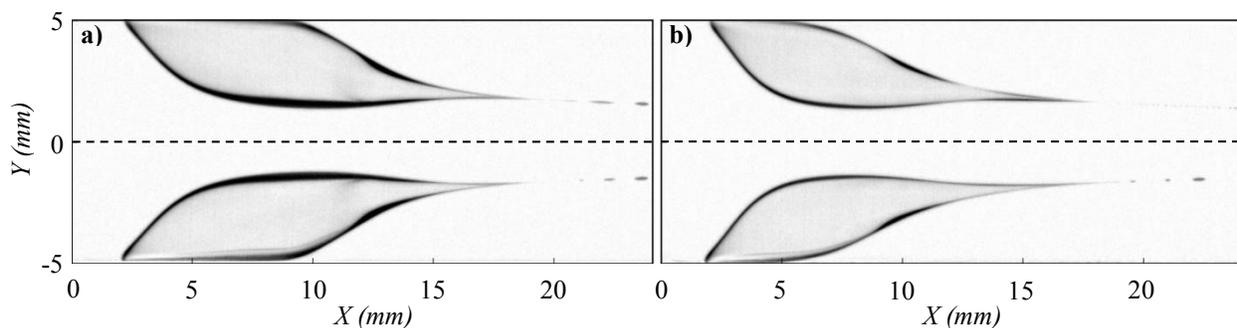

Figure 5 – Two typical "tadpole" bubbles observed with a top view for (a) $Re = 450$ and $\sigma = 42$ and for (b) $Re = 500$ and $\sigma = 34$.

In these two regimes micro-bubble sheddings can be observed, such as in figure 4 and 5. These sheddings, that occur with high frequencies, might be due to the gas diffusion [6] of the dissolved air present in the flow at interface of bubbles. This mechanism induces the growth of a bubble until a critical size leading to the shedding.

5. Conclusions

In the present paper, a first overview about the different cavitation regimes in laminar flows ($350 < Re < 1000$) has been made and the outcomes have been compared to the usual dynamical regimes observed into water-turbulent cavitating flows. The following summarizes the important conclusions.

- Two different gaseous cavitation dynamical regimes have been identified in the laminar flow, namely the **bubbly recirculation** and the **tadpole regime**.
- The inception of cavitation in the oil is similar to that one observed into water with the intermittent regime except that the bubbles generated do not condensate (and implode) in higher pressure regions, due to the high viscosity of the oil.
- The study of cavitation inception and desinence reveals a **hysteresis** which induces the tadpole regime.
- The two regimes are characterized by **two critical Reynolds numbers**, $Re_c^d \approx 350$ and $Re_c^i \approx 650$, which represent hydrodynamic transitions: namely the disappearance of the recirculation region and the emergence of an adverse pressure gradient at the throat.

6. Future Developments

In an upcoming article, the cavitation inception will be highlighted with top and side visualizations while the two regimes exposed in this paper will be characterized with the measurements of bubble sizes and shedding frequencies depending on cavitation and Reynolds numbers. In a meantime other dynamical regimes will be investigated for higher velocity inlet and thus higher Reynolds numbers. The first observations suggest the inception of a second bubbly recirculation zone at the top of the Venturi as well as a transition from gaseous to classical vaporous cavitation for higher Reynolds numbers.

Acknowledgement

References

[1] Brandner, P. A., Pearce, B. W., de Graaf, K. L. (2015). *Cavitation about a jet in crossflow*. J. Fluid Mech. Vol. 768, pp. 141-174.

[2] Croci, K., Tomov, P., Ravelet, F., Danlos, A., Khelladi, S., Robinet, J.-C. (2016). *Investigation of two mechanisms governing cloud cavitation shedding: experimental study and numerical highlight.* ASME Int. Mech. Eng. Congress and Exposition, *Volume 7: Fluid Engineering.*

[3] Ganesh, H., Mäkiharju, S. A., Ceccio, S. L. (2016). *Bubbly shock propagation as a mechanism for sheet-to-cloud transition of partial cavities*. J. Fluid Mech. Vol. 802, pp. 37-78.

[4] Brennen, C. E. (1995). *Cavitation and bubble dynamics*. Oxford University Press, New York.

[5] Washio, S., Takahashi, S., Yoshimori, S. (2003). *Study on cavitation starting at the point of separation on a smooth wall in hydraulic oil flow*. Proc. Inst. Mech. Eng., Part C: J. Mech. Eng. Science Vol. 217, pp. 619-630.

[6] Gross, T. F., Pelz, P. F. (2017). *Diffusion-driven nucleation from surface nuclei in hydrodynamic cavitation*. J. Fluid Mech. Vol. 830, pp. 138-174.